Sedimentary Geology, 32 (1982) 1—26
Elsevier Scientific Publishing Company, Amsterdam — Printed in The Netherlands

PLIO-PLEISTOCENE LACUSTRINE STROMATOLITES FROM LAKE TURKANA, KENYA: MORPHOLOGY, STRATIGRAPHY AND STABLE ISOTOPES

PAUL I. ABELL [1], STANLEY M. AWRAMIK [2], ROBERT H. OSBORNE [3] and STERLING TOMELLINI [1]

[1] *Chemistry Department, University of Rhode Island, Kingston, RI 02881 (U.S.A.)*
[2] *Department of Geological Sciences, University of California, Santa Barbara, CA 93106 (U.S.A.)*
[3] *Department of Geological Sciences, University of Southern California, Los Angeles, CA 90007 (U.S.A.)*

(Received July 6, 1981; revised and accepted October 26, 1981)

ABSTRACT

Abell, P.I., Awramik, S.M., Osborne, R.H. and Tomellini, S., 1982. Plio-Pleistocene lacustrine stromatolites from Lake Turkana, Kenya: morphology, stratigraphy and stable isotopes. Sediment. Geol., 32: 1—26.

A sequence of fossil stromatolites from Lake Turkana in Kenya was examined for $\delta^{18}O$ and $\delta^{13}C$ content. These stromatolites, ranging in age from Holocene (~10,000 yrs B.P.) to Middle Pliocene (~3 m.y.) showed a variety of growth forms from oncolitic, columnar layered to bulbous heads. The stromatolites used in our study contain filamentous blue-green algae of one morphological type and rare coccoids; thus the stromatolites are considered biogenic. The stable isotope ratios for oxygen and carbon indicate changing climatic conditions, ranging from a cool, wet climate prior to ca. 1.9 m.y. to much drier, warmer conditions around 1.4 m.y., followed in turn by a somewhat cooler and wetter climate at the end of the Pleistocene.

INTRODUCTION

The measurement of stable isotope ratios in naturally occurring materials has become a valuable source of information on the origin and paleoenvironmental history of these materials. In particular, $\delta^{18}O$ measurements on carbonates frequently are being used to elucidate climatic conditions prevailing at the time of deposition of these carbonates. Foraminifera, molluscs and other calcareous fossils have been studied, and climatic histories in varying detail now extend back into the Cretaceous (Savin, 1977). Particularly complete climatic histories for the recent geologic past has been derived from Greenland and Antarctic ice cores (Epstein et al., 1970), and older histories from Deep Sea Drilling Project marine cores using calcareous nannoplankton

0037-0738/82/0000—0000/$02.75

(Margolis et al., 1975). Nonmarine stromatolites previously have not been investigated for paleoclimatic information using the calcite presumably deposited as a by-product of the photosynthetic activity of their algal builders. Well developed stromatolites with preserved blue-green algal microfossils are found at different stratigraphic levels in Plio-Pleistocene lacustrine sedimentary deposits of the lake ancestral to modern Lake Turkana in Kenya. Owing to the rarity of detrital grains in the stromatolitic laminae, the stromatolites accreted by the precipitation of calcium carbonate. Assuming that the deposition of the calcite in these stromatolites was in equilibrium with the CO_2 in the lake water in which the algae grew, a stable isotope study of these stromatolites could define the climatic history of that lake. Climatic information derived from such studies has particular importance because these same sedimentary sequences probably contain the richest source of Plio-Pleistocene hominid fossils presently known (Coppens et al., 1976) and thus any paleoenvironmental information from this region may assist in explanation of the relatively rapid evolutionary progression of *Homo* and ancestral forms as well as other vertebrates in this area.

METHODS

From two to twenty intact and solid interior fragments of stromatolites were collected for isotopic studies from each of seven beds. The intact stromatolites were slabbed with a diamond saw and the slabs were then sampled at intervals of 2—5 mm for the isotopic analyses. The remainder of each slab was used for biogeologic, petrographic and petrochemical studies.

The fragments selected for isotopic analyses were baked at 400—450°C in vacuum for four hours to remove any organic material, and weighed samples (5—7 mg) then were dissolved in 100% phosphoric acid on a standard vacuum line to liberate the carbon dioxide. Isotope ratios were measured on a V.G. Micromass 602 ratio recording mass spectrometer, using a second standard for comparison. All isotope ratios are reported vs. PDB.

GEOLOGIC SETTING

Lake Turkana (until recently known as Lake Rudolf) lies in the Great Rift Valley of northern Kenya. The lake has existed since Miocene time, but most of the volcanics and sediments exposed around the lake are of Plio-Pleistocene age (Bowen and Vondra, 1973). The present-day lake is alkaline, with a pH of about 9.5 (Beadle, 1932), but at various times in the past, it has been freshwater (based on fossil fauna), overflowing through a shallow depression to the northwest to eventually reach the White Nile. A tectonic history of the lake has been proposed by Cerling and Powers (1977).

Much of the current interest in Lake Turkana arises from the discovery of a large number of well preserved homonid fossils along its northeast shores (Leakey, 1976). Some of these fossils date back as much as three million years, and are accompanied by artifacts (stone tools) as old as two million years (Coppens et al., 1976).

Geologic studies in the East Turkana area were imitiated by Behrensmeyer (1970) and continued by Vondra et al. (1971), Bowen and Vondra (1973) and by Findlater (1976), as well as others. The Plio-Pleistocene sequences consist of a complex of alluvial fan, fluvial, deltaic and lacustrine deposits exposed over an area approaching 2600 km^2 (White and Harris, 1977). These deposits have been correlated using a series of volcanic tuff deposits (Bowen and Vondra, 1973), which have been dated by conventional K-Ar and $^{40}Ar/^{39}Ar$ total degassing geochronologic methods (see Fitch and Miller, 1976). The radiometric ages are very critical to establishing the timing of evolutionary events in hominid phylogeny.

Bowen and Vondra (1973) divided the East Turkana Plio-Pleistocene succession into four formations; from oldest to youngest: (1) Kubi Algi Formation, exposed principally in the southernmost part of the region; (2) the Koobi Fora Formation, subdivided into lower and upper members; (3) the Guomde Formation, deposited unconformably on the Koobi Fora Formation, and identifiable principally in the most northern portion of the expo-

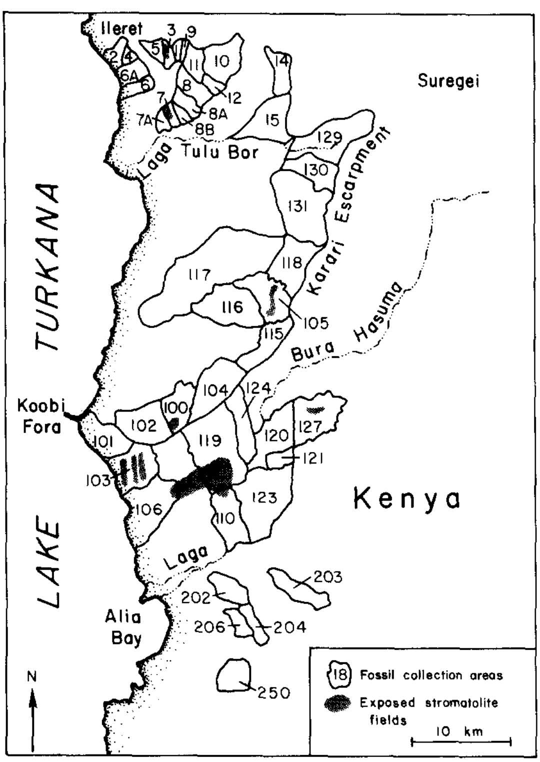

Fig. 1. Map of East Turkana, Kenya, showing topographic collecting areas and regions of exposed stromatolite fields.

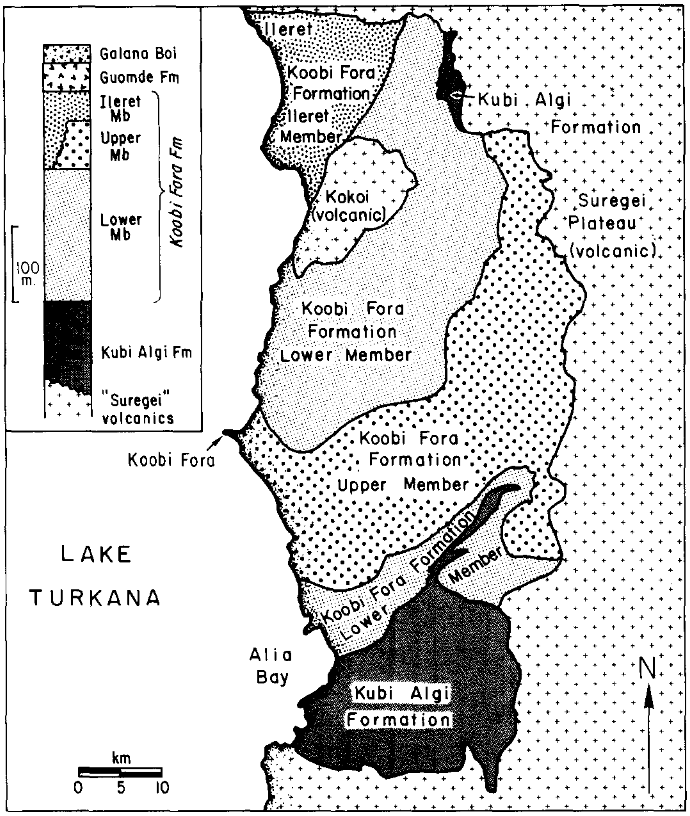

Fig. 2. Generalized geologic map of northeast shore of Lake Turkana, Kenya.

sures at Ileret; and (4) the Galana Boi beds, widely distributed in residual patches on the older sediments (Figs. 1 and 2).

The Pliocene Kubi Algi Formation at its type locality 20 km east of Alia Bay consists of a 98 m thick sequence of basal light colored cobble conglomerate vertically grading into sandstone, siltstone and claystone (Bowen, 1974). Two tuffs within the Kubi Algi yield isotopic ages of 3.9 and 4.6 m.y. (Fitch and Miller, 1976). These predominantly coarse-grained strata lie unconformably on Miocene or Pliocene volcanics and are conformably overlain by laminated bentonitic tuffs and claystone of the Suregei Tuff Compplex (Bowen and Vondra, 1973). No radiometric dates are available for the Suregei Tuff (Fitch and Miller, 1976).

The Koobi Fora Formation stratigraphically lies between the basal contact of the Suregei Tuff Complex and the upper contact of the Chari and Karari Tuff (isotopically dated at 1.3 m.y.; Fitch and Miller, 1976) or, at Ileret, between the basal contact of Holocene diatomaceous siltstone of the Galana Boi beds (Vondra and Bowen, 1976). The Koobi Fora Formation has been subdivided into two members: The Lower Member (that portion below the disconformity just above the KBS Tuff) and the Upper Member with its correlative strata at Ileret (the Ileret Member) found above the KBS tuff (Bowen and Vondra, 1973). The age of the KBS tuff has been the subject of considerable controversy. Fitch and Miller (1976) assign an isotopic age of 2.4 m.y., while Curtis et al. (1975) date it as young as 1.8 m.y., but most of Curtis et al. dates cluster around 1.9 m.y. The recent fission track date of Gleadow (1980) and the K-Ar date of McDougall et al. (1980) both confirm the 1.9 m.y. age of that tuff, and have settled the controversy. The Lower Member (>1.9 m.y.) reaches a thickness of 140 m and is characterized by alternating limonitic siltstone and claystone, ripple-laminated sandstone, and molluscan limestone (Vondra and Bowen, 1976). The Upper Member (<1.9 m.y.) is 90 m thick at Koobi Fora and consists of trough cross-bedded sandstone and conglomerate intercalated with siltstone, stromatolites, and ostracod sandstone. The Ileret Member (maximum thickness of 66 m) consists of homogeneous fine-grained sandstone and siltstone geographically restricted to Ileret ridge (Vondra and Bowen, 1976).

The Guomde Formation, restricted to Ileret ridge, is 34 m thick and consists of dark gray laminated siltstone with intercalated thin molluscan limestone. It overlies the Chari Tuff and underlies the diatomaceous siltstone of the Galana Boi beds (Vondra and Bowen, 1976).

The Galana Boi beds are the uppermost stratigraphic unit in East Turkana. These diatomaceous siltstones cap the Guomde Formation in the Ileret area and the Koobi Fora Formation further south (Vondra and Bowen, 1976). Thickness of the Galana Boi at Ileret is less than a meter but the strata thicken to as much as 32 m at Koobi Fora (Bowen, 1974).

STROMATOLITES FROM EAST TURKANA

The stromatolites from East Turkana are widely distributed, both laterally and vertically in Koobi Fora, Guomde and Galana Boi strata. They were first reported by Vondra et al. (1971) and later Johnson (1974) discussed details of their stratigraphic distribution and outlined their possible paleoecological significance. The oldest stromatolite bed we have identified from East Turkana to date occurs near the base of the Lower Member of the Koobi Fora Formation just a few meters below the Tulu Bor Tuff in Area 127 (Figs. 2 and 3; Sample *S*). No stromatolites have been positively identified from the underlying Kubi Algi Formation. At present, we wish to report on stromatolites from seven distinct horizons at East Turkana and discuss them in terms of the major fossil collecting areas in which they occur (Figs. 1 and 3). It should be noted that the stratigraphic position of Sample *R*, Area 119, is uncertain (Fig. 2).

(1) Area 127 has one stromatolitic unit bed (Sample *L*) in the basal portion of the Lower Member, Koobi Fora Formation. These algally-coated limonite clast stromatolites form a distinct bed within a 1 m thick coarse sand

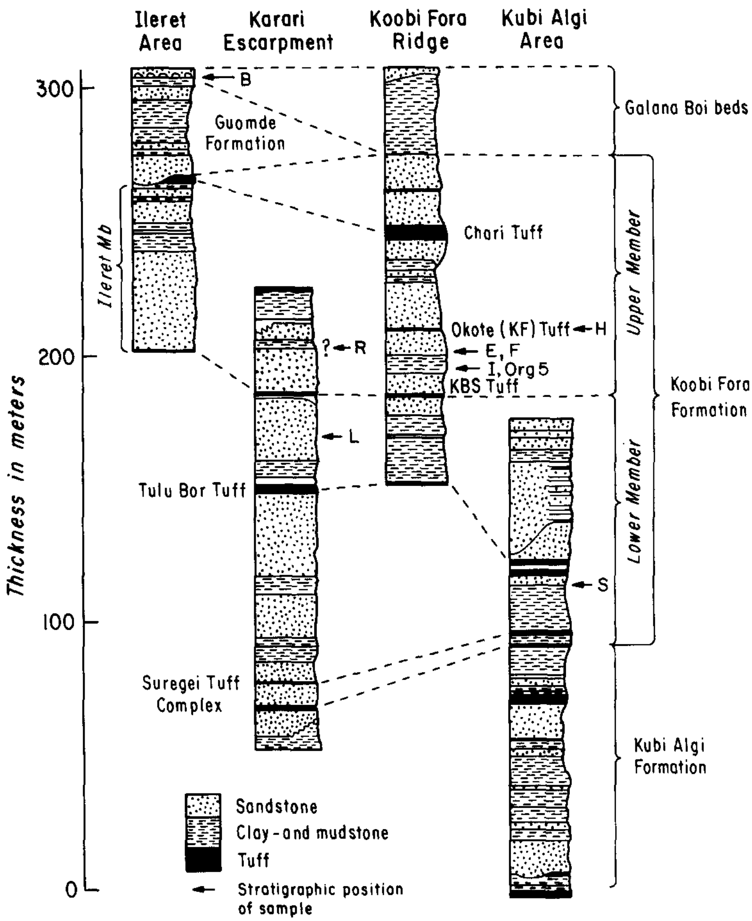

Fig. 3. Generalized stratigraphic section of East Turkana basin showing presumed correlative tuff units from north (left) to south (right) (modified from Bowen and Vondra in Vondra and Bowen, 1976) and approximate levels at which stromatolites used in this study were collected.

layer, but laterally can be traced into chaotically arranged stromatolite clasts (Fig. 4F). This unit is limited laterally in extent, and crops out for only a few hundred meters. The algally coated clasts are neatly arranged in one plane, long axes of clasts parallel to bedding. These probably formed in a small lake embayment rather than in a stream, as there is no evidence (disrupted or eroded laminae, asymmetric growth) to indicate a high degree of turbulence accompanying growth).

(2) Stromatolites in Area 105 (Sample *L*) and related areas occur above the Tulu Bor Tuff and are similar in morphology to Area 127 forms, except here they also coat gastropod shells. This outcrop in the Lower Member of the Koobi Fora Formation at Area 105 extends laterally for about 2 km; data

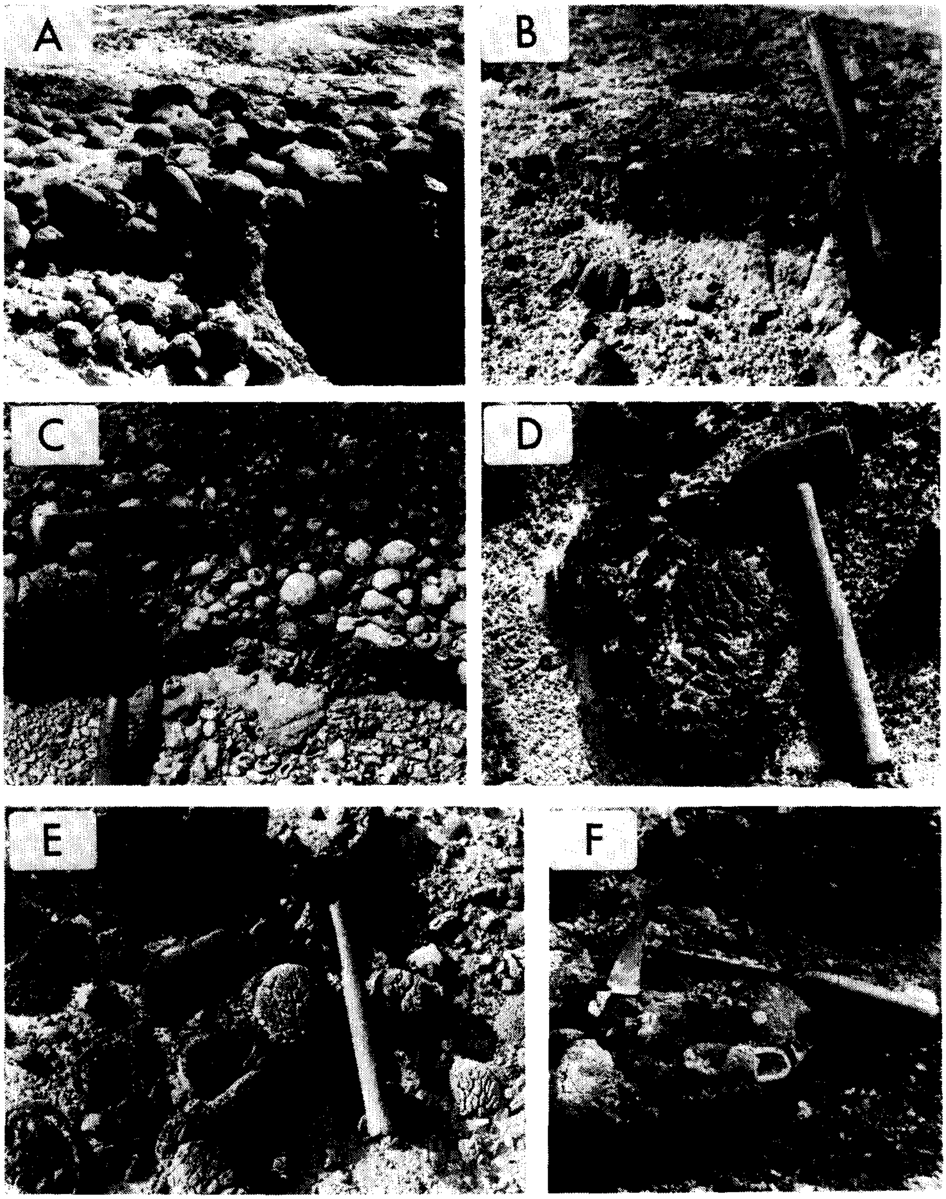

Fig. 4. Field occurrences of Lake Turkana stromatolites. A. Area 5 next to Area 3; Galana Boi beds; B. Area 103 branched mini-columns similar to Sample *E*, Upper Member, Koobi Fora Formation; C. Area 103 oncolites, Upper Member, Koobi Fora Formation; D. Area 103 large bulbous head, Upper Member, Koobi Fora Formation; E. Area 103 small bulbous heads similar to Samples *I* and *Org 5*, Upper Member, Koobi Fora Formation; F. Area 127 stromatolite coated limonite fragments similar to Sample S, Lower Member, Koobi Fora Formation.

are unavailable to determine overall geometry of the deposit. Thin, distinct beds 2—5 cm thick are found where the stromatolites coat gastropod shells. In contrast, the coated limonite fragments are somewhat chaotically arranged within a 1 m thick bed of coarse-grained sand.

(3) In Area 103, three distinct stromatolite beds are found in the Upper Member, Koobi Fora Formation, several meters above the KBS Tuff. The uppermost bed (from which Sample *H* was collected) is within the Okote (*KF*) Tuff horizon. These three beds crop out over an area of several tens of km^2, and probably extend into Areas 100, 101, 106, 110, and 119 (Fig. 3), though this correlation is tentative. The lowest bed, only 10 to 20 cm thick, is made up of diacontinuous bulbous stromatolite heads that seldom coalesce (Samples *I* and *Org 5*). The middle bed, never more than 20 cm thick, is made up of closely-spaced bulbous stromatolites (Samples *E* and *F*; Figs. 4D and E). This bed is prevalent and distinctive, and consequently serves as the principle correlative bed in Area 103. The stromatolites from this middle bed are made of two distinct layers and the following generalities can be made: (1) stromatolites in lower portions of each bed commonly coat mollusc fragments (both bivalves and gastropods) and form a thin bed several centimeters thick. The bivalves are disarticulated with valve concavity random and together with gastropods form a loose molluscan 'pavement'. Each molluscan shell is algally coated to form an oncolite (Fig. 4C). There is no evidence, aside from the enclosing sand, that these oncolites formed in a turbulent environment, considered normal, for oncolite formation (Logan et al., 1964). No eroded, truncated, or otherwise disrupted laminae were observed. Laminae are continuous but asymmetric around the molluscan nucleus, and each lamina consistently thickens on the upper surface. This preferential thickening in one direction with truncation probably indicates in-situ formation. In-situ oncolite growth is known from Pennsylvania streams (Roddy, 1915), where maximum laminar thickness is on the lower side (probably due to erosion of the upper side by stream action; Golubic and Fischer, 1975). The Turkana oncolites do not show micro-unconformities within the laminae; therefore, they probably were not subject to much abrasion; (2) oncolite beds laterally link upwards thus forming the substrate upon which grew bulbous stromatolites. The boundary between the two growth modes is sharp. Bulbous forms widen upward and adjacent heads interfere with bulbous expansion or lateral growth, resulting in polygonal shapes in the upper portion of these stromatolites. Bedding surfaces appear as mud-cracked polygons (Johnson, 1974) when actually the polygons are due to growth interference and crowding conditions during bulbous growth. Desiccation cracked silt and claybeds are widespread in Area 103 (Behrensmeyer, 1975) but are not found within the stromatolite beds. The top stromatolite bed (Sample *H*) consists of small nodular stromatolites, less than 10 cm long, and a few centimeters thick with convoluted upper surfaces. This bed is only a few centimeters thick and is patchy in distribution. Planar or undulose stratiform stromatolites are not well developed in East Turkana,

and this appears to be generally true of many non-marine stromatolites.

Area 103 stromatolite beds do not thin or thicken noticeably over any distance, and, considering the areal distribution of the stromatolitic horizons (particularly the middle horizon), might have grown in a shallow, flat embayment of the ancient lake. Based on sedimentological data, Behrensmeyer (1975) interpreted Area 103 to represent a deltaic mud flat to distributary channel complex.

(4) The stratigraphic position of stromatolites in Area 119 (Sample *R*) is uncertain, but the stromatolites are contiguous with these in Area 106. Indications are that these beds are nearly continuous for more than 15 to 25 km^2. The stromatolites vary in morphology from flattened bulbous heads, a few centimeters in diameter, to large nodules 1 m across. They are similar to those found in the Galana Boi beds at Ileret described below.

(5) The youngest stromatolites (Sample *B*) of the East Turkana succession are in basal Galana Boi beds at Areas 3, 5 and 7 (Fig. 3). These mollusc-stromatolite bearing beds yield ^{14}C ages on molluscs of 10,000 yrs B.P. (Vondra et al., 1971). Nodular (oncolitic) stromatolites, 1 cm to in excess of 0.5 m across, are found in lens-shaped beds a few tens of meters in width (Fig. 4A). Each nodule has a molluscan nucleus. Commonly the smaller nodules occur at the edges of the sedimentary lens and encrust *Caelatura* while the larger nodules in the center of the lens encrust single or gregarious *Etheria* (the common river oyster).

There are a few additional small outcrops of stromatolites at other stratigraphic levels at East Turkana but the details and stratigraphic position of these beds are unstudied.

PALEOMICROBIOLOGY OF THE STROMATOLITES

All stromatolites used in our study contain varying amounts of microfossils of presumed blue-green algal affinities but of low taxonomic diversity (Table I). Only two types have been found within the stromatolitic laminae: (1) abundant, non-branching, small filamentous forms, 0.8 to 4.3 μm across (21 measured) found only in Samples *L* and *Org 5*; and (2) small solitary coccoids measuring 2 to 5.3 μm in diameter (15 measured) found in Sample *R*.

The filamentous microfossils invariably are oriented perpendicular to laminae (Figs. 5B and C) and only in rare cases do they contain a single. centrally located thread (Fig. 5G). We interpret these filaments with their narrow size range as representing preserved sheaths of a single taxon of nostocalean blue-green algae with rare single trichomes. Insufficient fine morphological details are preserved to further refine our taxonomic treatment such as individual cells along the trichome; heterocysts, if present; and nondegradational tapering. The spheres, which occur solitary are single walled (no evidence of double walls or multi-layered sheaths), are of a narow size range, and probably represent a single taxon of a chroococcalean

TABLE I

Summary of isotope and stromatolite data

Sample	Area	Stratigraphy	Stromatolite morphology	Fabric and microstructure	Microfossils	Range of isotope ratios (PDB) *	
						$\delta^{18}O$	$\delta^{13}C$
B	3	base of Galana Boi	nodular (oncolite)	branched mini-colums, columnar-layered, with banded microstructure	non-branching filaments 1.2—4.3 μm	+0.8 to +2.2	—0.3 to +0.3
H	103	U. Mb. Koobi Fora Fm. Okote tuff	nodular (oncolite)	columnar-layered with banded microstructure	non-branching filaments 1.9—3.1 μm	+0.6 to +3.1	—0.8 to +0.3
E	103	U. Mb. Koobi Fora Fm. below Okote Tuff	encrusting-bulbous	branched mini-columns with poorly banded grumose microstructure	non-branching filaments 1.7—2.7 μm	—0.7 to +1.4	—0.2 to +1.4
F	103	U. Mb. Koobi Fora Fm. below Okote Tuff	bulbous	branched mini-colums with branched microstructure	non-branching filaments 0.8—3.9 μm	+2.1 to +3.3	—0.4 to +0.6
I	103	U. Mb. Koobi fora Fm. above KBS Tuff	bulbous	branched mini-columns with poorly banded, grumose microstructure	non-branching filaments 1.4—3.4 μm	+2.5 to +3.8	—0.2 to +1.1
Org-5	103	U. Mb. Koobi Fora Fm. above KBS Tuff	bulbous	branched mini-columns with poorly banded, dom. grumose microstructure	non-branching filaments 1.4—3.4 μm; rare coccoids 2.3—4.7 μm	+2.7 to +3.8	—0.2 to +0.8
L	105	L. Mb. Koobi Fora Fm. below KBS Tuff	nodular (oncolite)	pseudocolumnar with two size categories of banding	non-branching filaments 1.6—3.4 μm	—1.6 to +1.1	—3.0 to —1.4
S	127	L. Mb. Koobi Fora Fm. below Tulu Bor Tuff	(nodular (oncolite)	columnar-layered with banded microstructure	non-branching filaments 2.3—3.1 μm	—3.3 to —0.4	—2.4 to —1.5
J	100	?L. Mb. Koobi Fora Fm.	non-stromatolitic	unlaminated	none	+3.5 to —2.0	—3.4 to +1.5
R	119	?U. Mb. Koobi Fora Fm.	nodular to bulbous	pseudocolumnar, banded and grumose	non-branching filaments 0.8—3.9 μm; rare coccoids 3.1—4.3 μm	+0.9 to +2.4	—0.8 to +0.6

* Ranges of isotope ratios are calculated not only from illustrated stromatolites (Fig. 5), but also from additional analyses reported in Table II.

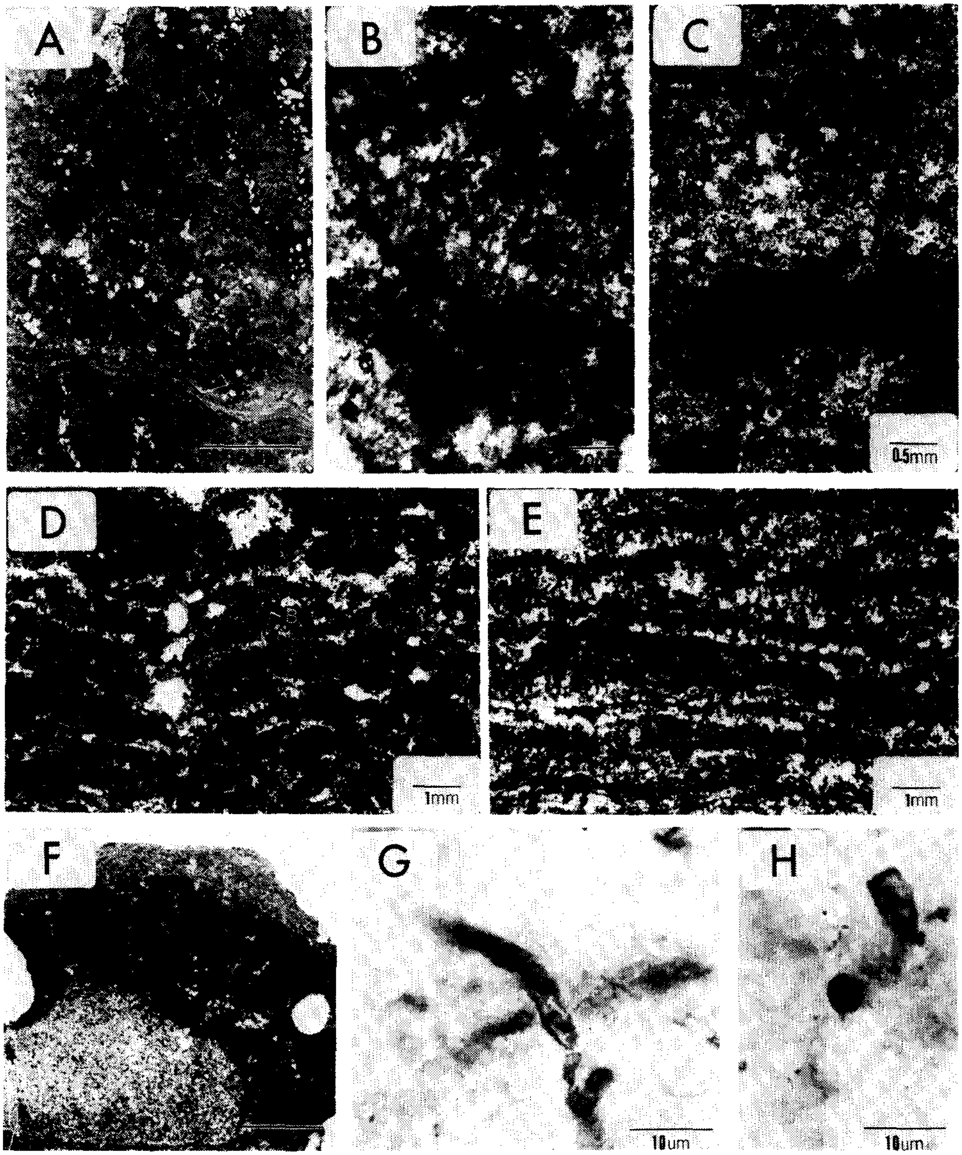

Fig. 5. Fabric, microstructure and microbiota of East Turkana stromatolites. A. Branched mini-columns with some columnar layering (arrows) in Sample *I*; B. Erect filamentous microfossils within poorly banded grumose microstructure in Sample *I*; C. Grumose microstructure with erect filaments in Sample *Org 5*; D. Pseudocolumnar fabric with banded microstructure of two size classes (arrow at A indicates thin alternating dark—light laminae; arrow at B indicates thicker alternating dark—light laminae), Sample *L*; E. Pseudocolumnar to stratiform fabric with banded to grumose microstructure. Sample *R*; F. Columnar-layered fabric, Sample *H*; G. Filament showing possible trichome within sheath, Sample *L*; H. Possible coccoid cyanophyte, Sample *R*.

blue-green alga. We cannot determine whether the coccoids are planktonic or benthic and therefore are uncertain of their role in stromatolite formation.

No meaningful variation in population size, density or morphologic variability was found in the East Turkana microbiota. The extremely low diversity, yet abundance of one type of filament could indicate either preferential preservation of one kind of microorganism over others or (and ?) the existence of an ecologically stressful environment during formation of the stromatolites inhibiting the growth and development of a diverse stromatolitic microbiota.

FABRIC AND MICROSTRUCTURE

Monty (1976, p. 193) proposed four-fold hierarchical arrangement of stromatolite characteristics: (1) stromatolite — the individual cryptalgal structure constituting the deposit; (2) fabric — the internal spacial properties of the stromatolite; (3) microstructure — the microscopic characteristics of internal properties; and (4) ultrastructure — the habit and arrangement of cryptocrystalline units. Microstructure includes: (a) grain to grain and crystal to crystal relationships; (b) laminar thickness; (c) relief along a single lamina (amplitude); and (d) distribution of organic matter and elements associated with organic matter (Semikhatov et al., 1979). The Lake Turkana stromatolitic fabric is very distinct in terms of both the microstructure and stromatolite macrostructure. Microstructural elements are arranged in such a way to form distinct mini-columnar, columnar-layered, and linked, closely-spaced pseudocolumnar internal structures (Fig. 5) which are not morphologically related to the shape assumed by the stromatolites themselves (macrostructure).

Mini-columns are small, discrete columns, 1 to 7 mm across, commonly branched and composed of stacked, convex, alternating dark and light colored laminae. Columnar-layered micromorphologies or fabrics, are composed of a repetitive sequence of laminated domes a few millimeters across, which display high inheritence and are laterally continuous. Laminae are thicker at the dome crests. Pseudocolumnar fabric refers to an undulatory arrangement of laterally-linked alternating dark and light, uniformly thick laminae with a high degree of inheritance.

The laminae that constitute the microstructure can be grouped into three categories based on appearance in thin section (Fig. 5A—F): (1) distinctly banded; (2) poorly banded; and (3) grumose. Distinctly banded microstructures exhibit continuous, well-defined parallel dark and light layers. Dark layers are micritic while light layers are usually composed of radial fibrous calcite. The dark-light colored boundary is distinct, only a couple of micrometers thick. Dark layers are commonly thicker (16—80 μm) than light layers (16—55 μm, averaging 40 μm). Distinctly banded microstructures are found in all three types of fabrics. In Sample *L*, there are two size classes of dark and light couplets (Fig. 5D). Poorly banded microstructures have indistinct banding, but are composed of alternating dark thicker micrite with thinner light, radial fibrous calcitic layers with some neomorphic calcite; the boundary between dark and light layers in diffuse, more like a transition taking place over several micrometers. The third style of microstructure is clotted or grumose usually made up of poorly defined layers composed of small grey pelloids, 50 to 90 μm across within a microspar matrix, alternating with light-colored sparite. Darker layers are commonly thicker (40—90 μm) than light layers (30—70 μm). Filamentous microfossils are found in all three microstructures.

Based on the non-detrital nature of the fabric and microstructure, all stromatolites in our study presumably formed by the in-situ precipitation of calcium carbonate.

STROMATOLITIC SEDIMENTS

The samples examined (only stromatolites, not enclosing matrix) average about 82.8% (by volume) of stromatolitic carbonate, 11.5% of empty, partly or wholly filled open-space structures, and 5.7% detrital and allochemical grains. Obvious detrital and allochemical grains range from 1.0 to 15.4% of the stromatolites by volume, but most often comprise from 4.0 to 6.0%. It is certain that these values are minimal, because they represent only those grains measurable at thin section scale. Iron oxide coatings and the high birefringence of carbonates undoubtedly mask very fine-grained silt and clay within stromatolitic laminae, micrite and microspar. Insoluble residue analyses on those samples of sufficient size indicate that the preceding values only represent from 40 to 60% (by weight) of the total insoluble residue present. The weight of insoluble residue does not include the weight of the organic material which was oxidized by a 12% solution of hydrogen peroxide prior to drying and weighing.

Bulk analysis of stromatolite samples *R*, *H*, and *B* by X-ray diffraction and atomic absorption indicated the presence of only low magnesium calcite (0.131 and 0.326 mole % $MgCO_3$). The magnitude of mineralogical and/or chemical differences between successive laminae was not determined.

The observed detrital grains range from fine-grained silt (0.008 mm) to very coarse-grained sand (1.25 mm), and predominantly occur between or among coalescing stromatolitic domes and within partly or wholly filled open-space structures in the stromatolites. In most samples the detrital grains range from medium-grained silt (0.016 mm) to medium-grained sand (0.05 mm) with modes in the fine- to medium-grained sand fraction (0.125—0.50 mm). The detrital grains range from very angular to rounded with rho values (Folk, 1955) from 0 to 5; however, they are generally from subangular to subrounded with rho values from 2 to 4. Sphericity values (Rittenhouse, 1943) range from 0.53 to 0.89, but generally range from 0.71 to 0.85.

The detrital component consists dominantly of undulatory (greater than 5 degrees of flat stage rotation) and nonundulatory monocrystalline quartz with subordinate polycrystalline quartz normally with two to three crystal units per grain. The feldspars are represented by orthoclase, microcline, and plagioclase ranging in composition from albite to labradorite but most frequently from oligoclase to andesine. Non-opaque accessory minerals are represented by normal hornblende, augite, zircon, tourmaline, biotite and rutile, whereas the opaque minerals are represented by magnetite-ilmenite and leucoxene. This detrital mineral assemblage suggests derivation from acid igneous and metamorphic source rock with a relatively minor contribution from basic igneous rocks. This conclusion compares favorably with that reached by Bowen (1974, p. 89) and Vondra and Bowen (1976, p. 87) who suggest the source area for the late Cenozoic strata in the Lake Turkana area was probably the Precambrian plutonic igneous and metamorphic complex exposed near the northern limit of Lake Stephanie in Ethiopia with local but sometimes predominant contributions from basaltic to rhyolitic volcanic terrains.

Intrabasinal allochems associated with the detrital grains include ooids, oncolites, mollusc and ostracod fragments, and structureless carbonate grains (peloids). The ooids are generally light brown. They are composed of calcite and display well-developed radial and concentric structure. Although some superficial ooids occur, most are multi-layered, normal ooids from 0.26 to 0.35 mm in diameter. Most of the ooids are developed on quartz or feldspar cores, but some have single or double peloidal cores. No offset nuclei were observed. Micrite rims may be present, but are masked by iron-oxide staining. The ooids do not display the protruding nuclei, asymmetry and scalloped edges suggestive of quiet-water formation (Freeman, 1962), nor do they have the desiccation cracks such as those described by Adeleye (1975). Thus there is little evidence to suggest subaerial exposure of the ooids. Oncolites consist of micritic laminae of calcite surrounding detrital grains of quartz, feldspar and micritic peloids. They are not common in the samples examined, but range in diameter from about 0.15 to 0.25 cm. Peloids occur as apparently spherical to subspherical micritic grains with no apparent internal structure. They range in diameter from 0.5 to 0.9 mm and are most likely fecal pellets of gastropods. These allochems invariably are mixed with extrabasinal detrital grains, which demonstrates that they are transported from sites of carbonate accumulation and deposited among and within stromatolitic encrustations during floods or storms.

MAJOR DIAGENETIC EFFECTS

Although the degree of diagenetic alteration may vary considerably within any given stromatolite, similar styles of diagenetic alteration are common to all of the stromatolites examined. The initial stromatolitic microstructure appears to be the repetition of a couplet composed of a dark-colored micritic

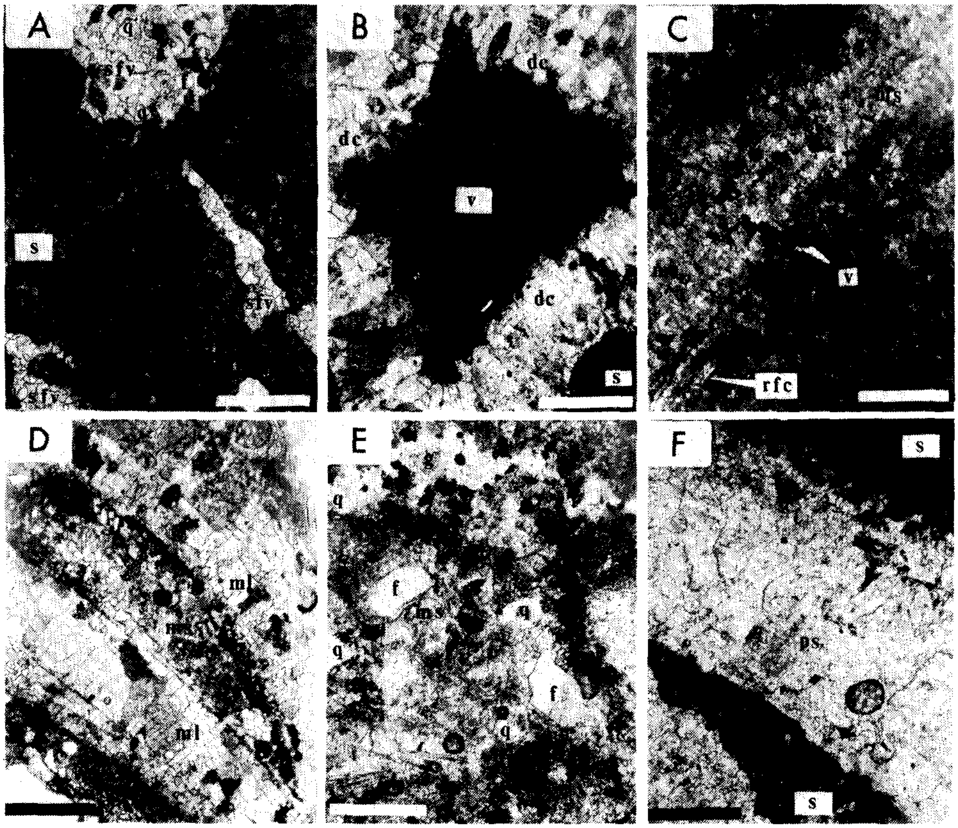

Fig. 6. Photomicrographs showing principal diagenetic features within the Lake Turkana stromatolites. Scale bars represent 0.5 mm. Abbreviations used: stromatolitic carbonate (*s*); detrital quartz grain (*q*); detrital feldspar grain; (*f*) sediment-filled void (sfv); void (*v*); drusy calcite (*dc*); microspar (*ms*); radial fibrous calcite (*rfc*); mollusc grain (*ml*); ghost structure (*g*); and pseudosparite (*ps*). A. Sediment-filled void (solution structure) within stromatolitic carbonate. Note detrital grains of quartz and feldspar floating in microspar. (Plane polarized light); B. Solution void lined with drusy calcite cement. (Cross polarized light); C. Laminae of radial fibrous calcite replaced by neomorphic microspar adjacent to and above prominent solution void. (Cross polarized light); D. Replacement of mollusc grains by blocky mosaic of calcite. Note occurrence of neomorphic microspar between mollusc grains (Plane polarized light); E. Detrital grains of quartz and feldspar floating in microspar probably represent an original detrital lamina disrupted by displacive neomorphism. Note ghost structure of ooid or peloid. (Plane polarized light); F. Set of stromatolitic laminae (lower left) detached from main stromatolite (upper right) by displacive neomorphism (Plane polarized light).

lamina and a light-colored lamina of radial fibrous calcite.

The following diagenetic processes have modified the initial stromatolitic structure during the evolution of these biosedimentary structures: dissolution, cementation, replacement, internal sedimentation and the disruption or displacement of stromatolitic laminae and any internal detrital structure by aggrading neomorphism. There is no evidence of subaerial desiccation structures within the stromatolitic carbonate or associated carbonate grains.

Small open-space structures as much as 0.10 mm high occur within the stromatolitic carbonate. These may represent voids formed by stromatolitic encrustations over irregular surfaces or by the decomposition of calcite-encrusted organic matter (Osborne et al., in press). Such voids may be enlarged by the dissolution of surrounding carbonate.

Large open-space structures (Fig. 6A) from 0.5 mm to 1 cm high probably formed by multiple episodes of carbonate deposition and solution within the stromatolites. This interpretation is suggested by the termination of stromatolitic laminae against these voids, the high degree of inheritance between successive laminae, and the likelihood that the calcitic laminae were hard when only a few millimeters thick. Moreover, the outer laminae are usually complete over the height of the stromatolites and do not show the deformation which might be expected where these large open-space structures due to laminae parting. It is also likely that organic matter which might supply gas for uplift of stromatolitic laminae rapidly decreases with depth. Therefore, this organic matter is not likely to yield much gas at any given time (Osborne et al., 1982).

The dissolution of stromatolitic carbonate which produced the large, open-space structures is one of the most obvious diagenetic effects. The resultant cavities as well as voids beneath and among mollusc grains are frequently either partly or wholly lined with clear, drusy calcite cement (Fig. 6B) with planar intercrystalline boundaries. Such linings often appear as geopetal fabrics.

These large, open-space structures as well as voids between and among coalescing domes may be filled with silt- and sand-sized detrital (Fig. 6A) and allochemical grains, sparite, micrite or any combination of these constituents.

Another obvious diagenetic modification observed in both the stromatolitic carbonate (Fig. 6C) as well as in void-filling micrite (Fig. 6A) is the embayment and replacement of these calcitic materials by microspar and pseudospar. Aggrading neomorphism is indicated by the replacement of mollusc grains (Fig. 6D) and the occurrence of detrital and allochemical grains floating in a mass of pseudospar. In several instances, it is likely that displacive neomorphism has disrupted detrital laminae (Fig. 6E) within solution voids and has displaced stromatolitic laminae away from the main stromatolitic dome (Fig. 6F).

It is clear that diagenetic alteration may start shortly after carbonate deposition (Osborne et al., 1982), and this is probably true for the Lake Turkana stromatolites. Diagenetic alteration in response to fluctuations in lake level, ground water and perhaps climatic factors have homogenized the stromatolites at the petrographic scale so that there are no obvious diagenetic trends with age.

ISOTOPIC RESULTS

The variations in $\delta^{13}C$ and $\delta^{18}O$ for each of the stromatolites studied are presented graphically in Fig. 8. All of the isotopic measurements are plotted in Fig. 7 as $\delta^{18}O$ vs. $\delta^{13}C$. Most of the results of the individual stromatolites fall into fairly narrow ranges of values for each stromatolites (Tables I and II). When the points scatter widely, as they do in some cases, it is usually because the particular fragment being analyzed is from the outside or is next to a void in the stromatolite and has been subjected to weathering.

The limonite-calcite cores of some stromatolite beds have different isotope ratios from the algal deposited coating (Sample S, Fig. 7B). Finally,

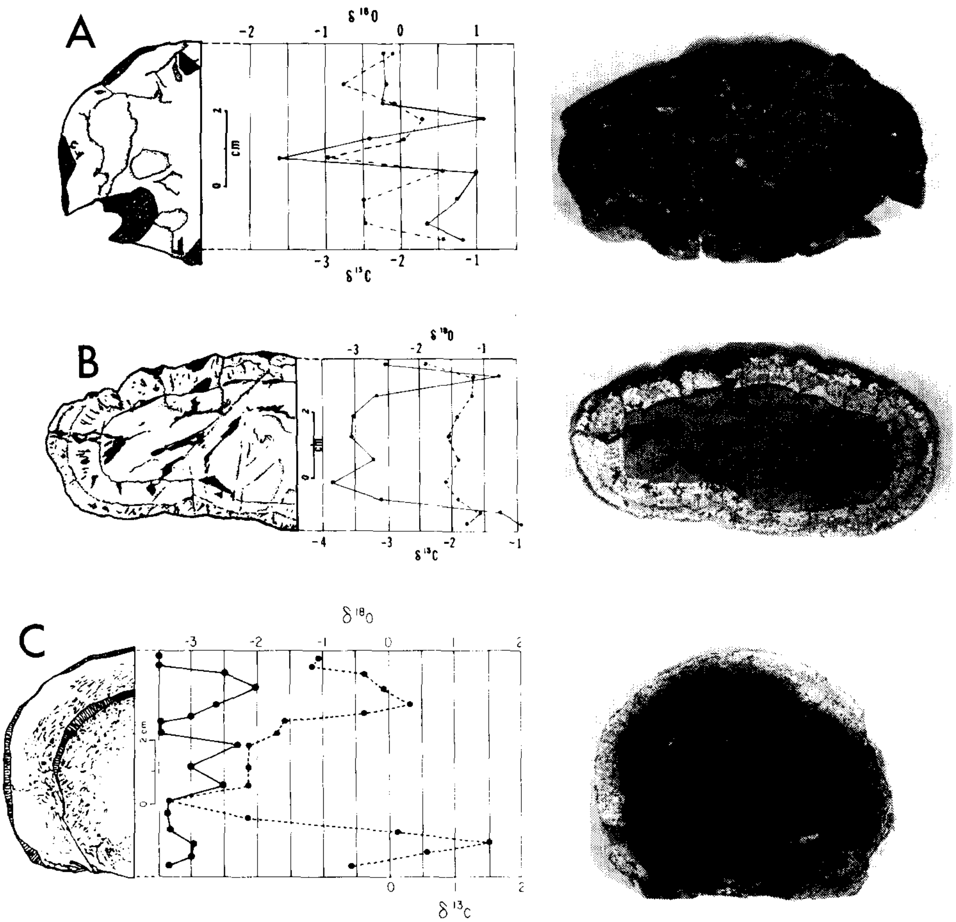

Fig. 7. Matched sets of specimen drawings, graphs illustrating $\delta^{18}O$ (solid line) and $\delta^{13}C$ (dashed line) and actual specimens for each sample studied in detail. Centimeter scale between left drawing and graph. A. Sample L, Area 105; B. Sample S, Area 127; C. Sample J, Area 100, the only non-stromatolite sample.

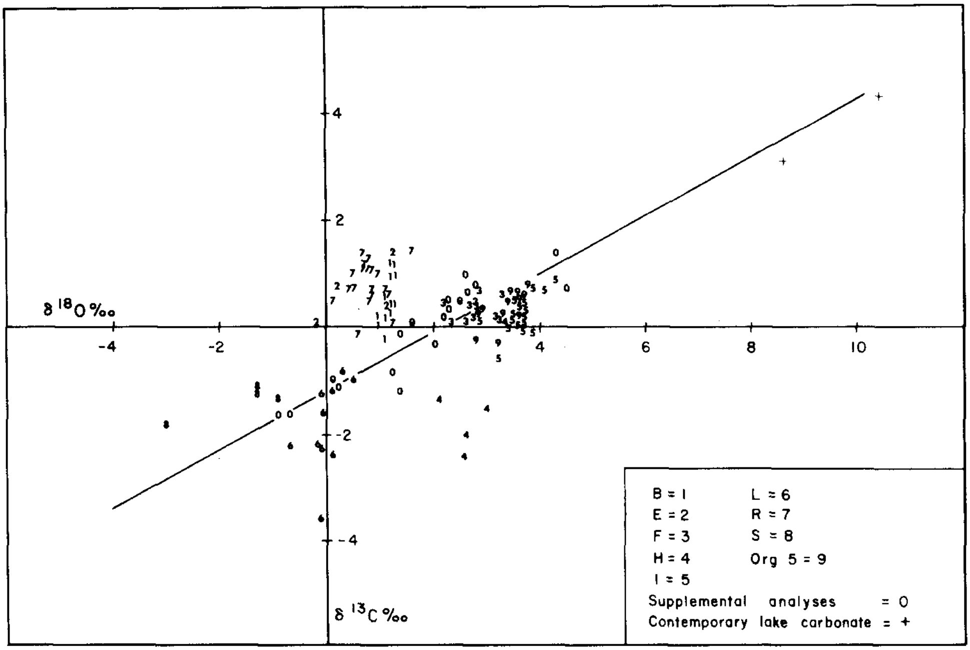

Fig. 8. All values of $\delta^{18}O$ vs. $\delta^{13}C$. Linear regression calculated for all samples except Sample *J* which is not stromatolitic and central part of Sample *S*, the limonite clast.

TABLE II

Bulk isotope analyses of additional selected stromatolites

Location of stromatolite bed	$\delta^{18}O$	$\delta^{13}C$ (PDB)
Area 3, Galana Boi beds	2.03	−0.28
	1.61	0.01
	1.26	−0.81
	1.37	−0.08
	1.38	−1.21
Area 103, upper algal unit	2.22	0.49
	2.29	0.38
	2.20	0.18
Area 103, middle algal unit	2.64	0.64
	2.61	1.03
	2.52	0.50
	2.87	0.85
Area 103, lower algal unit	4.32	1.38
	3.50	0.61
	4.47	0.78
Area 105, sub KBS Tuff	−0.90	−1.60
	−0.62	−1.65
Area 127, sub Tulu Bor Tuff	0.09	−1.08
	0.17	−1.13

many of the stromatolites at Lake Turkana formed on shells of various molluscan species. The isotope ratios for these shells need not bear any relationship to the isotope ratios of the algal calcite, because the calcites of stromatolite and mollusc not necessarily having been deposited under identical lake conditions. Despite these difficulties, if solid, relatively unaltered stromatolites are selected for analysis and interior fragments chosen with care and taken as characteristic of the growth period for that stromatolite, it is possible to obtain meaningful values of $\delta^{18}O$ and $\delta^{13}C$ for each bed (Tables I and II). These values fall along a straight line, as shown in Fig. 8, with a slope of 0.56 and an intercept at −1.22 on the $\delta^{13}C$ axis.

The variation of oxygen isotope ratio with climatic conditions is well known (see Emiliani, 1970; Margolis et al., 1975). Under warm, dry conditions rain water is fractionated as it falls, with the water reaching the ground enriched in the heavier isotope of oxygen. Evaporation of the lake waters will also leave behind the heavier isotope. The $\delta^{18}O$ values thus increase with arid conditions, and conversely, decrease during cool, wet periods. The fact that the source of most of the water for the Lake Turkana basin is in the highland areas of Ethiopia and to a lesser extent Uganda means that local evaporation will have a more pronounced effect on $\delta^{18}O$ than the conditions prevailing where the rain fell. Figure 9 illustrates these changes with a particularly large climatic change taking place at about the time of the deposition of the KBS Tuff. It is significant to note, our data also indicate that the Turkana stromatolites formed under both arid and cool and wet conditions.

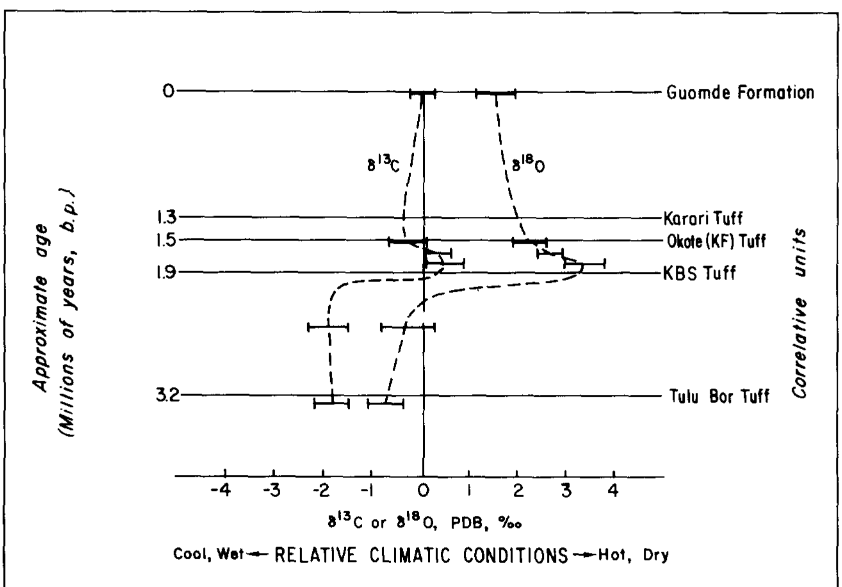

Fig. 9. Variation of $\delta^{18}O$ and $\delta^{13}C$ with age as derived from dated volcanic tuffs.

The close parallel between carbon and oxygen isotope oscillations (Figs. 7, 10 and 11), suggests that the carbon and oxygen which have gone to form the stromatolite have been in close equilibrium with their environment. Whatever the detailed habitat in which the stromatolites grew, the carbon and oxygen were subjected to similar fractionations. With oxygen we believe the principal fractionating force is evaporation of water, concentrating the

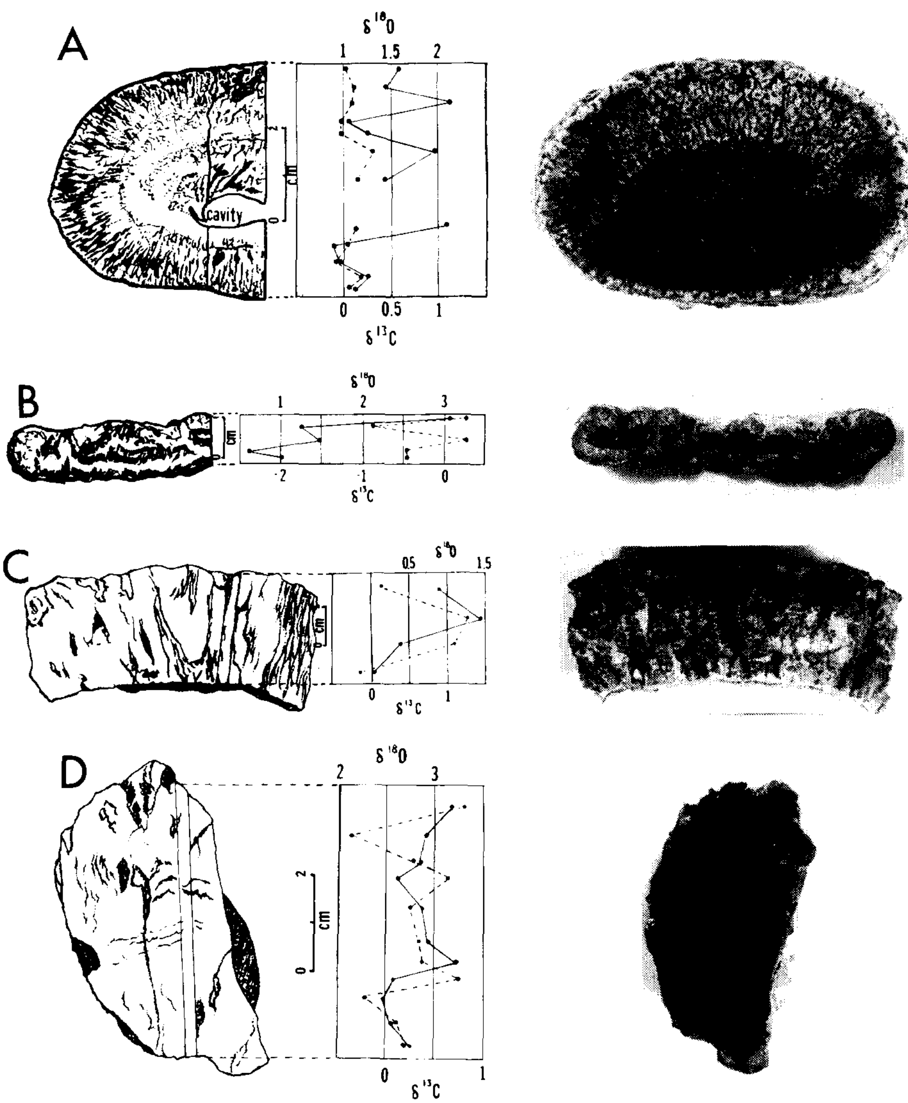

Fig. 10. Matched sets of specimen drawings, graphs illustrating $\delta^{18}O$ (solid line) and $\delta^{13}C$ (dashed line), and actual specimens for each sample studied in detail. Centimeter scale between left drawing and graph. A. Sample *B*, Area 3; B. Sample *H*, Area 103; C. Sample *E*, Area 103; D. Sample *F*, Area 103.

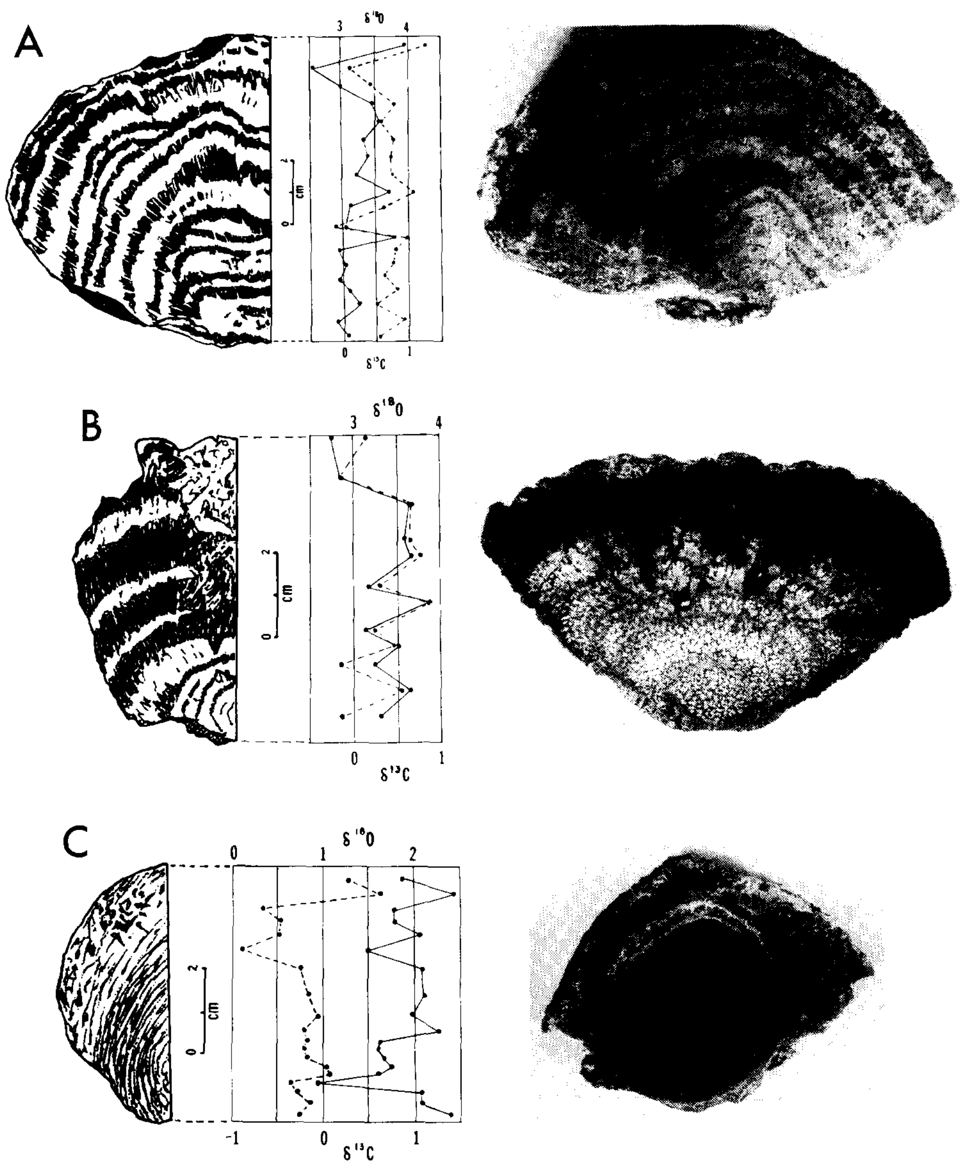

Fig. 11. Matched sets of specimen drawings, graphs illustrating $\delta^{18}O$ (solid line) and $\delta^{13}C$ (dashed line), and actual specimens for each sample studied in detail. Centimeter scale between left drawing and graph. A. Sample *I*, Area 103; B. Sample *Org 5*, Area 103; C. Sample *R*, Area 119.

heavy oxygen in the liquid phase. The fractionation of carbon isotopes cannot follow a similar route because there is believed to be no fractionation between atmospheric carbon dioxide and dissolved carbon dioxide (Degens, 1969; Deins and Gold, 1973). But there is a major fractionation between dissolved CO_2 and bicarbonate ion, enriching the latter by about 7 to 10 per mil in the heavier isotope. Thus, one possible explanation for the increase in ^{13}C under arid conditions is an increasing reservoir of heavy dissolved carbonate as the lake grows more alkaline. This hypothesis can be tested by isotopic examination of carbonate deposits, including stromatolites, in the varied alkalinities of the rift valley lakes of Kenya and Tanzania.

There are still enormous gaps in our ability to interpret the isotope data. There is little isotopic difference between the stromatolites below the Tulu Bor Tuff up to the pre-KBS Tuff level. This is a period during which the lake was fresh, and filled to overflow level (Cerling and Powers, 1977). Then above the KBS Tuff level, there is a shift to much more positive $\delta^{18}O$ and $\delta^{13}C$ values, characteristic of a much drier, hotter climate. This climatic change is reflected in the changes in fossil vertebrates and molluscs, in the geochemistry of tuff weathering, in the pollen trapped in the sediments. A drift toward more negative isotope ratios is recorded in successive stromatolite beds of Area 103 as the lake rose in a cooler, wetter period. There is then, unfortunately, a break in the continuity of sedimentary beds through much of the Pleistocene, until the Holocene. Presumably, there would be a whole sequence of oscillations between wet and dry, cool and hot periods, were the carbonate isotope information available. The "early" Holocene climate is fairly cool and wet, which is verified by other evidence of a moderate climate in the Sahara region at the end of the most recent glaciation. There are no known deposits of stromatolites at Lake Turkana since that time, so we cannot compare modern conditions with the ancient using a modern stromatolite. The carbon and oxygen isotopic content of the modern lake in terms of dissolved carbonates is very much more positive than the Galana Boi (10,000 yrs B.P.) stromatolites, so that presumably the trend lines in Fig. 9 would veer sharply to the right were stromatolites being formed today, reflecting the much more arid conditions and warmer climate of today. The degree of isotopic fractionation between the water carbonate and the stromatolite carbonate is unknown.

It is interesting to compare the climatic data elucidated from stable carbon and oxygen isotope content of these stromatolites with other evidence of climatic change. We have observed a major change of climate from cool, wet to warm, dry conditions at about the time of deposit of the KBS Tuff, i.e, about 1.9 m.y. ago. Cerling et al. (1977) have examined the oxygen isotope ratios of pedogenic calcretes and nodules and carbonate nodules (non-stromatolitic) from lacustrine clays from sediments at Lake Turkana and they observe a shift in $\delta^{18}O_{SMOW}$ values of 26.3—27.9 (—4.2 to -2.6_{PDB}) below the KBS Tuff, to 30.4—33.0 (—0.2 to $+2.3_{PDB}$) above that tuff. A similar change in $\delta^{18}O$ was noted by these authors at Olduvai Gorge on similar carbonate sediments. There, the change in oxygen isotope ratio comes at the end of the deposition of Bed I, which would put the date of major climatic change at about 1.7 m.y.

There are sources of information other than isotope ratios. For example.

Cerling et al. (1977) observe that the weathering of volcanic ash below the KBS tuff (to montmorillonite) differs from weathering of ash above that tuff (to montmorillonite, chabazite and clinoptilolite). The latter products are indicative of a hot, dry climate with alkaline, saline lake conditions, while formation of the montmorillonite alone is a fresh water alteration product of volcanic ash.

Harris (1976) notes a change in the fossil bovid population at the KBS Tuff level, implying a change in climate or ecology. A similar change in species population occurs in the fossil fauna at the Omo River between Members G and H, dated at 1.8—1.9 m.y. (Coppens and Howell, 1976).

Palynology has also demonstrated a substantial change in climate at the KBS Tuff level. Bonnefille has looked at the pollen assemblage from the sedimentary deposits of both Lake Turkana (Bonnefille, 1976a) and the Omo Basin (Bonnefille, 1976b). In both cases, the pollen at pre-KBS Tuff levels is characteristically highland and riverine in plant types, while the post-KBS Tuff pollen assemblage is from plants characteristic of a savanna environment.

Finally, Williamson (1978) has carried out an extensive study of the fossil mollusc population of the Lake Turkana sediment, and he too finds a sharp break in the occurrence of many species at the KBS Tuff level. Six of the twenty-two mollusc species he identified become extinct at that time, suggesting a change in ecological conditions inferred to be related to climatic change. Gautier (1976) also notes changes in the fossil mollusc population on the Omo Basin, but does not see quite such an abrupt change as Williamson (1978).

There is little doubt but that there was a major change in climate in the Rift Valley in northern Kenya about 1.9 m.y. ago from cooler, wetter conditions to hotter and drier conditions. It is interesting to speculate on and would be even more interesting to measure the change in climate that took place in the Rift Valley of Africa during the remainder of the Pleistocene with the advances and retreats of the glaciers further north. Unfortunately, that sedimentary history is incomplete in the deposits at Lake Turkana. More intensive searches of the Guomde beds for stromatolites would be highly desirable, and the stable isotope study of other calcareous deposits in the sediments might be productive. Stable isotope studies of the mollusc population and the diatoms are planned. In addition, we plan to investigate other lakes and basins along the Great Rift in Kenya and Tanzania that have stromatolites and other calcareous deposits. Eventually, it should be possible to develop a detailed climatic history of the Great Rift Valley and relate that to man's evolution in this part of Africa.

SUMMARY AND CONCLUSIONS

Stromatolites have been extensively used in paleoecological analyses of ancient marine settings, however their value as determinants of ecological conditions in ancient nonmarine environments have not been fully explored. Our study of Middle Pliocene to Holocene stromatolites from lake deposits ancestral to Lake Turkana, Kenya may be summarized as follows:

(1) Meaningful oxygen and carbon isotopic data are possible from biogenic stromatolites which have not undergone severe diagenetic alteration. Such studies at Lake Turkana indicate a change in climatic conditions from cool and wet prior to about 1.9 m.y. ago to dry and warm around 1.4 m.y. ago followed in turn by somewhat cooler, moister conditions at the end of the Pleistocene.

(2) The stromatolites formed in a variety of physical settings from fluviatile to lacustrine, turbulent to non-turbulent; no single environmental setting appears to have been favored.

(3) Though morphologies are extremely variable, the preserved blue-green algal microbiota presumed responsible for stromatolite formation is similar in all stromatolites, regardless of morphology, age or environmental setting.

(4) The differences in microstructure found in the stromatolite cannot be correlated with differences in the preserved microbiota or gross morphology.

(5) The gross morphology assumed by a stromatolite cannot be correlated with any particular characteristic of the physical environment. We do not know what controls macrostructure.

ACKNOWLEDGEMENTS

We would like to acknowledge the assistance of the following persons in making this research possible: Lloyd Kiegwin and Michael Bender of the Graduate School of Oceanography, University of Rhode Island, for making a mass spectrometer available; Donald Hermes of the Geology Department, University of Rhode Island, for assistance in Mg/Ca ratio determinations: Melinda Marian, University of Southern California for X-ray diffraction and atomic absorption analyses on stromatolites samples; Duncan Dow, Mines and Geology Department, Kenya, for assistance in slabbing the specimens; Ian Findlater, Resident Geologist, National Museum, Kenya, for assistance in field geology; and especially to R.E. Leakey and G.L. Isaac for making available the facilities of the base camp at Lake Turkana. Valuable comments on early drafts of this manuscript were provided by T.E. Cerling (Oak Ridge), J. Kennett (U.R.I.), T.L. Ku and E. Grossman (U.S.C.).

Contribution No. 91, Biogeology Clean Laboratory, University of California, Santa Barbara; Contribution No. 373, Department of Geological Sciences, University of Southern California.

REFERENCES

Adeleye, D.R., 1975. Derivation of fragmentary oolites and pisolites from desiccation cracks. J. Sediment Petrol., 45: 794—798.

Beadle, L.C., 1932. The waters of some East African lakes in relation to their fauna and flora. J. Linn. Soc. London, Bot., 38: 135—156.

Behrensmeyer, A.K., 1975. The taphonomy and paleoecology of Plio-Pleistocene vertebrate assemblages east of Lake Rudolf, Kenya. Bull. Mus. Comp. Zool., 146: 473—578.

Bonnefille, R., 1976a. Implication of pollen assemblages from the Koobi Fora Formation, East Rudolf, Kenya. Nature, 264: 403—407.

Bonnefille, R., 1976b. Palynological evidence for an important change in the vegetation of the Omo basin between 2.5 and 2 million years ago. In: Y. Coppens, F.C. Howell, G.L. Isaac and R.E.F. Leakey (Editors), Earliest Man and Environments in the Lake

Bonnefille, R., 1976b. Palynological evidence for an important change in the vegetation of the Omo Basin between 2.5 and 2 million years ago. In: Y. Coppens, F.C. Howell, G.L. Isaac and R.E. Leakey (Editors), Earliest Man and Environments in the Lake Rudolf Basin. University Chicago Press, Chicago, Ill., pp. 421—431.

Bowen, B.E., 1974. The geology of the Upper Cenozoic Sediments in the East Rudolf Embayment of the Lake Rudolf Basin, Kenya. Thesis, Iowa State University, Ames, Iowa, 164 pp. University Microfilms, Ann Arbor, Mich., 74—23, 723.

Bowen, B.E. and Vondra, C.F., 1973. Stratigraphical relationships of the Plio-Pleistocene deposits, East Rudolf, Kenya. Nature, 242: 391—393.

Cerling, T.E. and Powers, D.W., 1977. Paleorifting between the Gregory and Ethiopian Rifts. Geology, 5: 441—444.

Cerling, T.E., Hay, R.L. and O'Neil, J.R., 1977. Isotopic evidence for dramatic climatic changes in East Africa during the Pleistocene. Nature, 267: 137—138.

Cerling, T.E., Cerling, B.W., Curtis, G.H., Drake, R.E. and Brown, F.H., 1978. Correlation of reworked ash deposits: the KBS Tuff, northern Kenya. 4th Int. Conf. Geochronology and Isotope Geology.

Coppens, Y. and Howell, F.C., 1976. Mammalian faunas of the Omo Group: distributional and biostratigraphical aspects. In: Y. Coppens, F.C. Howell, G.L. Isaac and R.E.F. Leakey (Editors), Earliest Man and Environments in the Lake Rudolf Basin. University of Chicago Press, Chicago, Ill., pp. 177—192.

Coppens, Y., Howell, F.C., Isaac, G.L. and Leakey, R.E.F., 1976. Earliest Man and Environments in the Lake Rudolf Basin. University Chicago Press, Chicago, Ill., 615 pp.

Curtis, G.H., Drake, R.E., Cerling, T.E., Cerling, B.W. and Hampel, J.H., 1975. Age of KBS Tuff in Koobi Fora Formation, East Rudolf, Kenya. Nature, 258: 395—398.

Degens, E.T., 1969. Biogeochemistry of stable carbon isotopes. In: G. Eglinton and M.T.J. Murphy (Editors), Organic Geochemistry. Springer, Berlin, pp. 304—329.

Deins, P. and Gold, D.P., 1973. The isotopic composition of carbonatite and kimberlite carbonates and their bearing on the isotopic composition of deep-seated carbon. Geochim. Cosmochim. Acta, 37: 1709—1733.

Emiliani, C., 1970. Pleistocene paleotemperatures. Science, 168: 822—825.

Epstein, S., Sharp, R.P. and Gow, A.J., 1970. Antarctic ice sheet: stable isotope analyses of Byrd Station cores and interhemispheric climatic implications. Science, 168: 1570—1572.

Findlater, I.C., 1976. Tuffs and the recognition of isochronous mapping units in the East Rudolf succession. In: Y. Coppens, F.C. Howell, G.L. Isaac and R.E.F. Leakey (Editors), Earliest Man and Environments in the Lake Rudolf Basin. University Chicago Press, Chicago, Ill., pp. 94—104.

Fitch, F.J. and Miller, J.A., 1976. Conventional potassium-argon and argon-40/argon-39 dating of volcanic rocks from East Rudolf. In: Y. Coppens, F.C. Howell, G.L. Isaac and R.E.F. Leakey (Editors), Earliest Man and Environments in the Lake Rudolf Basin. University Chicago Press, Chicago, Ill., pp. 123—147.

Folk, R.L., 1955. Student operator error in determination of roundness, sphericity and grain size. J. Sediment. Petrol., 25: 297—301.

Freeman, T., 1962. Quiet water oolites from Laguna Madre, Texas. J. Sediment. Petrol., 32: 475—483.

Gautier, A., 1976. Assemblages of fossil freshwater mollusks from the Omo Group and related deposits in the Lake Rudolf basin. In: Y. Coppens, F.C. Howell, G.L. Isaac and R.E.F. Leakey (Editors), Earliest Man and Environments in the Lake Rudolf Basin. University Chicago Press, Chicago, Ill., pp. 379—382.

Gleadow, A.J.W., 1980. Fission track age of the KBS tuff and associated hominid remains in northern Kenya, Nature, 284: 225—230.

Golubic, S. and Fischer, A.G., 1975. Ecology of calcareous nodules forming in Little Connestoga Creek near Lancaster, Pennsylvania. Verh. Int. Ver. Limnol., 19: 2315—2323.

Harris, J.M., 1976. Bovidae from the East Rudolf succession. In: Y. Coppens, F.C. Howell, G.L. Isaac and R.E.F. Leakey (Editors), Earliest Man and Environments in the Lake Rudolf Basin. University Chicago Press, Chicago, Ill., pp. 293—301.

Johnson, G.D., 1974. Cainozoic lacustrine stromatolites from hominid-bearing sediments east of Lake Rudolf, Kenya. Nature, 247: 520—523.

Leakey, R.E., 1976. An overview of the Hominidae from East Rudolf, Kenya. In: Y. Coppens, F.C. Howell, G.L. Isaac and L.E.F. Leakey (Editors), Earliest Man and Environments in the Lake Rudolf Basin. University Chicago Press, Chicago, Ill., pp. 476—483.

Logan, B.W., Rezak, R. and Ginsburg, R.N., 1964. Classification and environmental significance of algal stromatolites. J. Geol., 72: 68—83.

Margolis, S.V., Kroopnick, P.M., Goodney, D.E., Dudley, W.C. and Magoney, M.E., 1975. Oxygen and carbon isotopes from calcareous nannofossils as paleooceanographic indicators. Science, 191: 1131—1137.

McDougall, I., Maier, R., Sutherland-Hawkes, P. and Gleadow, A.J.W., 1980. K-Ar age estimate for the KBS tuff, E. Turkana, Kenya. Nature, 284: 230—234.

Monty, C.L.V., 1976. The origin and development of cryptalgal fabrics. In: M.R. Walter (Editor), Stromatolites, Elsevier, Amsterdam, pp. 193—259.

Osborne, R.H., Licari, G.R. and Link, M.H., 1982. Modern lacustrine stromatolites, Walker Lake, Nevada. Sediment. Geol., 32: 39—61.

Rittenhouse, G., 1943. A visual method of estimating two dimensional sphericity. J. Sediment. Petrol., 13: 79—81.

Roddy, H.J., 1915. Concretions in streams formed by the agency of blue-green algae and related plants. Proc. Am. Philos. Soc., 54: 246—258.

Savin, S.M., 1977. The history of the Earth's surface temperature during the past 100 million years. Annu. Rev. Earth Planet. Sci., 5: 319—355.

Semikhatov, M.A., Gebelein, C.D., Cloud, P., Awramik, S.M. and Benmore, W., 1979. Stromatolite morphogenesis — progress and problems. Can. J. Earth Sci., 16: 992—1015.

Vondra, C.F. and Bowen, B.E., 1976. Plio-Pleistocene deposits and environments, East Rudolf, Kenya. In: Y. Coppens, F.C. Howell, G.L. Isaac and R.E.F. Leakey (Editors), Earliest Man and Environments in the Lake Rudolf Basin. University Chicago Press, Chicago, Ill., pp. 79—93.

Vondra, C.F., Johnson, G.D., Behrensmeyer, A.K. and Bowen, B.E., 1971. Preliminary stratigraphical studies of the East Rudolf basin. Nature, 231: 245—248.

White, T.D. and Harris, J.M., 1977. Suid evolution and correlation of African hominid localities. Science, 198: 13—21.

Williamson, P., 1978. Plio-Pleistocene mollusc assemblages from east of Lake Turkana, north Kenya: an introduction. In: W.W. Bishop (Editor), Geological Background to Fossil Man. Scottish Academic Press, Aberdeen, pp. 507—527.